AD-A083 687 OHIO STATE UNIV COLUMBUS ELECTROSCIENCE LAB F/G 9/5
ON GRATING NULLS IN ADAPTIVE ARRAYS.(U)
MAR 80 A IGNIDE, R T COMPTON N00019-79-C-0281
UNCLASSIFIED ESL-711647-6 NL

END
DATE FILMED
6-80
DTIC

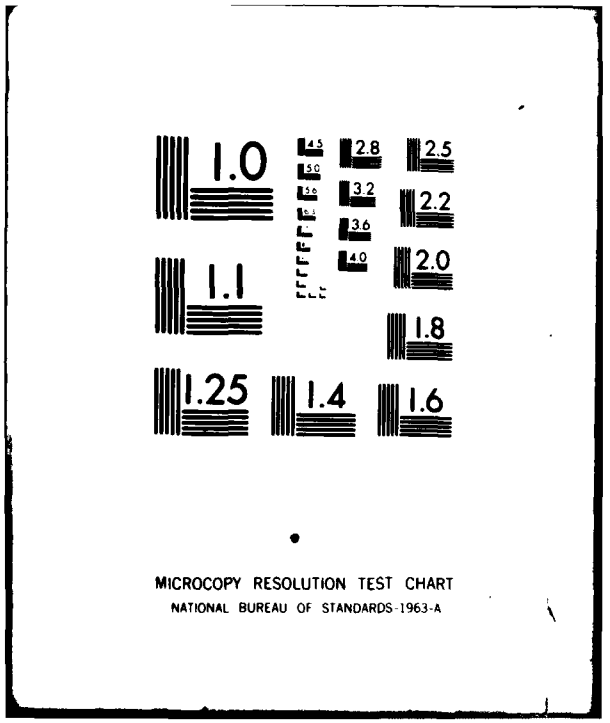
1.0
1.1
1.25
1.4
1.6
1.8
2.0
2.2
2.5
2.8
3.2
3.6
4.0
4.5
5.0
5.6
MICROCOPY RESOLUTION TEST CHART
NATIONAL BUREAU OF STANDARDS-1963-A

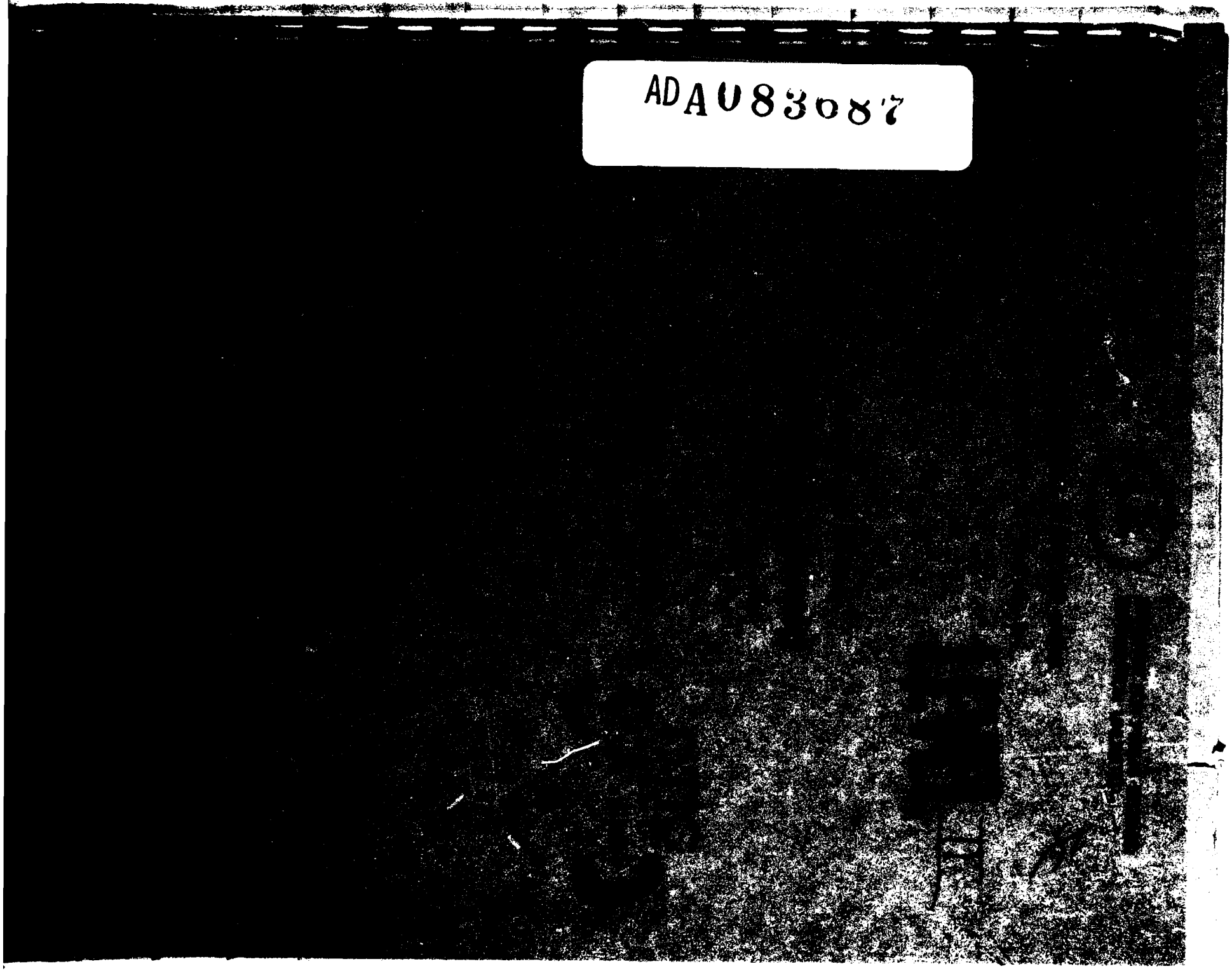

[redacted]

[redacted] specifications, or other data are [redacted] definitely [redacted] the United States [redacted] responsibility or any obligation [redacted] by implication, or otherwise as [redacted] any other person or corporation, [redacted] or yell [redacted] may in any way be related thereto.

SECURITY CLASSIFICATION OF THIS PAGE (When Data Entered)

REPORT DOCUMENTATION PAGE

READ INSTRUCTIONS BEFORE COMPLETING FORM

1. REPORT NUMBER

2. GOVT ACCESSION NO. AD-A083 687

3. RECIPIENT'S CATALOG NUMBER

4. TITLE (and Subtitle)

(6) ON GRATING NULLS IN ADAPTIVE ARRAYS

5. TYPE OF REPORT & PERIOD COVERED (9) Technical Report

6. PERFORMING ORG. REPORT NUMBER (14) ESL-711847-6

7. AUTHOR(s)

(10) A. Ishide and R. T. Compton, Jr.

8. CONTRACT OR GRANT NUMBER(s) (15) Contract N00019-79-C-0281

9. PERFORMING ORGANIZATION NAME AND ADDRESS
The Ohio State University ElectroScience Laboratory, Department of Electrical Engineering
Columbus, Ohio 43212

10. PROGRAM ELEMENT, PROJECT, TASK AREA & WORK UNIT NUMBERS

11. CONTROLLING OFFICE NAME AND ADDRESS
Naval Air Systems Command
Washington, D.C. 20361

12. REPORT DATE (11) March 1980

13. NUMBER OF PAGES

14. MONITORING AGENCY NAME & ADDRESS(if different from Controlling Office) (12) 38

15. SECURITY CLASS. (of this report)
Unclassified

15a. DECLASSIFICATION DOWNGRADING SCHEDULE

16. DISTRIBUTION STATEMENT (of this Report)

APPROVED FOR PUBLIC RELEASE:
DISTRIBUTION UNLIMITED

17. DISTRIBUTION STATEMENT (of the abstract entered in Block 20, if different from Report)

18. SUPPLEMENTARY NOTES

Accession For	
NTIS GRA&I	☐
DDC TAB	☐
Unannounced	☐
Justification	
By	
Distribution/	
Availability Codes	
Dist	Avail and/or special
A	

19. KEY WORDS (Continue on reverse side if necessary and identify by block number)
Adaptive Arrays
Antennas
Interference Rejection
Grating Nulls
Element Patterns

20. ABSTRACT (Continue on reverse side if necessary and identify by block number)

This report considers the effect of element patterns on grating nulls in adaptive arrays. Two simple array models, a two-element and a three-element array with dipole element patterns, are used to study this question. The element patterns are assumed unequal (i.e., the beam maxima point in different directions).

It is shown that element patterns greatly affect the occurrence of grating nulls in the array. Unequal element patterns cause extra grating nulls

DD FORM 1 JAN 73 1473 EDITION OF 1 NOV 65 IS OBSOLETE

402251

SECURITY CLASSIFICATION OF THIS PAGE (When Data Entered)

20. Abstract (continued).

("sign reversal grating nulls") to occur, in addition to conventional grating nulls. These sign reversal grating nulls can occur even with element spacing less than a half-wavelength. For a two-element array with dipole element patterns, it turns out that grating nulls cannot be avoided if the spacing is greater than a half wavelength. However, with more than two elements, the situation is not so bleak. An example is given of a three-element array with dipole patterns and one wavelength spacing in which all grating nulls are eliminated.

CONTENTS

I. INTRODUCTION

It is well known that an array with elements more than a half wavelength apart is subject to grating lobe effects. In the context of adaptive arrays, grating lobe effects manifest themselves in the form of spurious nulls. That is, interference nulled by the array at one angle may cause additional nulls ("grating nulls") at other angles. If the desired signal is near a grating null, the output signal-to-noise ratio from the array will be poor.

The purpose of this report is to examine the effects of element patterns on grating nulls in an adaptive array. We will use a simple model, an array with dipole element patterns, to show several things. First, we will find, as one would expect, that unequal element patterns in the array tend to reduce the effects of grating nulls. Second, however, we will also find that unequal element patterns can create other spurious nulls, in addition to conventional grating nulls. We will refer to these additional nulls as sign reversal grating nulls. Third, we will find that for a two-element array with dipole element patterns, it is impossible to avoid grating nulls for spacings greater than a half wavelength. But finally, we will show that grating nulls can be avoided by using more than two elements, if the element patterns are chosen properly.

We note that the case of unequal element patterns in an adaptive array is a case of great practical interest. An attractive feature of adaptive arrays is that a designer may locate elements somewhat arbitrarily on a structure. For example, antennas for aircraft communication may be placed at convenient locations on the aircraft. However, when this is done, the element patterns will usually be different. Moreover, one will often want to space the elements more than a half wavelength apart.

In Section II of the report, we formulate the problem of an N-element linear array with arbitrary element patterns. We assume desired signal, interference and thermal noise signals present in the array, and determine the output signal-to-interference-plus-noise ratio (SINR) from the array. In Section III we consider a specific array, a two-element array with dipole element patterns. We determine the conditions under which grating nulls occur and show that such an array always suffers from grating nulls if the spacing exceeds one-half wavelength. In Section IV, we use a three-element array with dipole element patterns and one wavelength element spacing to illustrate that grating nulls can be avoided with more than two elements. Finally, Section V contains our conclusions.

II. FORMULATION OF THE PROBLEM

Consider an N-element adaptive array, as shown in Figure 1. The elements are assumed to lie along a straight line with spacing d_j between element j and element 1. The complex signal $\tilde{x}_j(t)$ from the j^{th} element is multiplied by a complex weight w_j and summed to produce the array output $\tilde{s}(t)$. In an LMS array [1,2], the steady-state weight vector $w = (w_1\ w_2\ \ldots\ w_N)^T$ is given by

$$w = \Phi^{-1}S, \tag{1}$$

where Φ is the covariance matrix

$$= E\{X^*X^T\}, \tag{2}$$

and S is the reference correlation vector,

$$S = E\{X^*\tilde{R}(t)\}. \tag{3}$$

In these equations, X is the signal vector,

$$X = (\tilde{x}_1(t)\ \tilde{x}_2(t)\ \ldots\ \tilde{x}_N(t))^T, \tag{4}$$

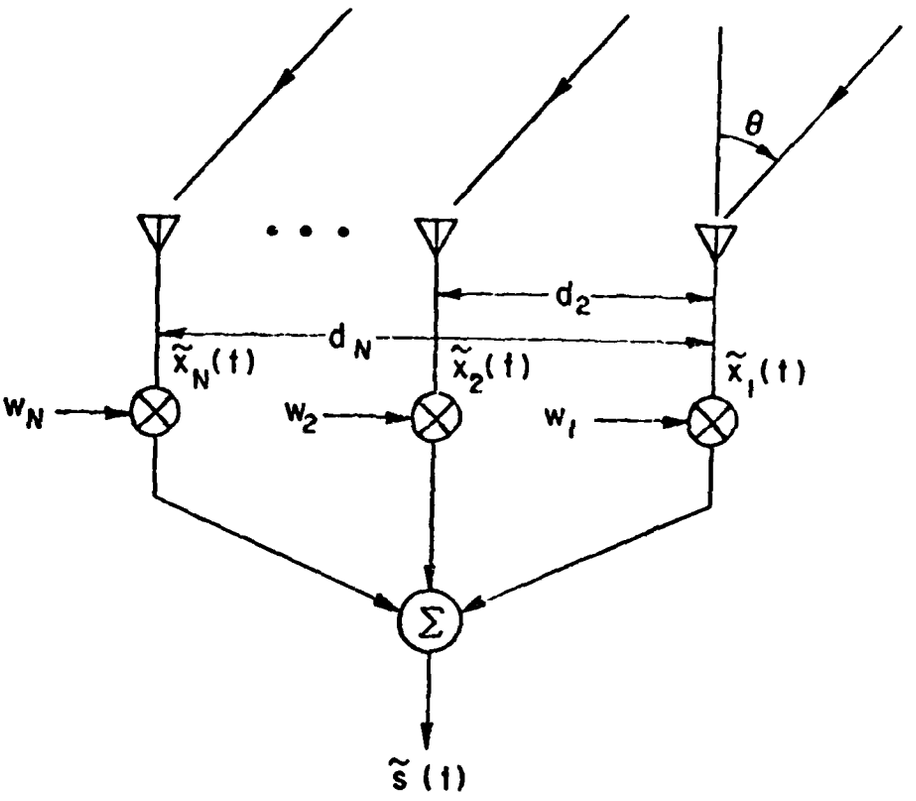

Figure 1. An N-element adaptive array.

$\tilde{R}(t)$ is the (complex) reference signal* in the adaptive array[3-6], T denotes transpose, "*" complex conjugate and $E(\cdot)$ expectation.

Assume two CW signals are incident on the array, one desired and the other interference. Let these signals arrive from angles θ_d and θ_i, respectively, with respect to broadside. Also, assume the j^{th} array element has voltage response $f_j(\theta)$ to a unit amplitude signal arriving from angle θ. Finally, assume thermal noise is present on each element signal. Then we have

$$\tilde{x}_j(t) = f_j(\theta_d)A_d e^{j(\omega_o t+\psi_d-\phi_{dj})} + f_j(\theta_i)A_i e^{j(\omega_o t+\psi_i-\phi_{ij})} + \tilde{n}_j(t), \tag{5}$$

where A_d and A_i are the amplitude of the desired and interference signals, ω_o is the signal frequency, ψ_d and ψ_i are the carrier phases, and $\tilde{n}_j(t)$ is the thermal noise. ϕ_{dj} is the desired signal interelement phase shift between element j and element 1,

$$\phi_{dj} = \frac{2\pi d_j}{\lambda} \sin \theta_d, \tag{6}$$

and ϕ_{ij} is the interelement phase shift for the interference,

$$\phi_{ij} = \frac{2\pi d_j}{\lambda} \sin \theta_i, \tag{7}$$

with λ the wavelength. We assume the noise signals $\tilde{n}_j(t)$ are zero mean, uncorrelated with each other, and have power σ^2:

$$E\{\tilde{n}_k^*(t)\tilde{n}_j(t)\} = \sigma^2\delta_{kj}, \tag{8}$$

---

*The reference signal is called the "desired response" in Widrow, et al. [1].

where δ_{kj} is the Kronecker delta. Also, we suppose the phase angles ψ_d and ψ_i are uniformly distributed on $(0,2\pi)$ and statistically independent of each other and the thermal noise.

Under these assumptions, the covariance matrix becomes

$$\Phi = \Phi_d + \Phi_i + \Phi_n, \tag{9a}$$

where

$$\Phi_d = E\{X_d^* X_d^T\} = A_d^2 U_d^* U_d^T, \tag{9b}$$

$$\Phi_i = E\{X_i^* X_i^T\} = A_i^2 U_i^* U_i^T, \tag{9c}$$

and

$$\Phi_n = \sigma^2 I . \tag{9d}$$

Here X_d is the desired signal vector,

$$X_d = A_d e^{j(\omega_o t + \psi_d)} U_d, \tag{10a}$$

with

$$U_d = \begin{pmatrix} f_1(\theta_d) \\ f_2(\theta_d) e^{-j\phi_{d2}} \\ \vdots \\ f_N(\theta_d) e^{-j\phi_{dN}} \end{pmatrix}, \tag{10b}$$

X_i is the interference signal vector,

$$X_i = A_i e^{j(\omega_o t + \psi_i)} U_i, \tag{11a}$$

with

$$U_i = \begin{pmatrix} f_1(\theta_i) \\ f_2(\theta_i)e^{-j\phi_{i2}} \\ \vdots \\ f_N(\theta_i)e^{-j\phi_{iN}} \end{pmatrix} , \tag{11b}$$

and I is the identity matrix.

To make the array track the desired signal, the reference signal must be a signal correlated with the desired signal and uncorrelated with the interference [5,6]. We assume

$$\tilde{R}(t) = A_r e^{j(\omega_o t+\psi_d)} . \tag{12}$$

Equation (3) then yields

$$S = A_r A_d U_d^* . \tag{13}$$

The steady-state weight vector w can now be found by substituting Equation (9) and (13) into Equation (1).

The signal-to-interference-plus-noise ratio (SINR) at the array output is then given by

$$SINR = \frac{P_d}{P_i+P_n} , \tag{14}$$

where P_d is the output desired signal power,

$$P_d = \frac{1}{2} E\{|X_d^T w|^2\} = \frac{A_d^2}{2} |U_d^T w|^2, \tag{15}$$

P_i is the output interference power,

$$P_i = \frac{1}{2} E\{|X_i^T w|^2\} = \frac{A_i^2}{2} |U_i^T w|^2, \tag{16}$$

and P_n is the output thermal noise power,

$$P_n = \frac{\sigma^2}{2} |w|^2. \tag{17}$$

It is shown in the Appendix that, by making use of a matrix inversion lemma, the SINR in Equation (14) can be expressed in the simple form:

$$\text{SINR} = \xi_d \left[U_d^T U_d^* - \frac{|U_d^T U_i^*|^2}{\xi_i^{-1} + U_i^T U_i^*} \right], \tag{18}$$

where we have defined

$$\xi_d = \frac{A_d^2}{\frac{\sigma^2}{2}} = \text{desired signal-to-noise ratio (SNR) on each element} \tag{19a}$$

$$\xi_i = \frac{A_i^2}{\frac{\sigma^2}{2}} = \text{interference-to-noise ratio (INR) on each element.} \tag{19b}$$

III. A TWO-ELEMENT ARRAY

We are interested in the SINR performance of an array with elements spaced wider than $\frac{\lambda}{2}$ apart, and in how the element patterns affect this performance. To gain an understanding of this problem, we will first consider a two-element array. Before including the element patterns, however, it is helpful to start with the case where the element patterns are isotropic: $f_1(\theta) = f_2(\theta) = 1$.

With isotropic elements, it is easily shown that if the desired signal arrives from angle θ_d, an interference signal at an angle

$$\theta_i = \sin^{-1}\left[\frac{n\lambda}{d} + \sin\theta_d\right], \quad n = \pm 1, \pm 2, \ldots \tag{20}*$$

will not only cause a null at θ_i, but will also cause a grating null at θ_d. Hence the desired signal will fall in this null and we may expect the output SINR to be poor.

Figure 2 shows an example of this behavior. The figure shows the output SINR from the array as a function of θ_i, for $d=\lambda$. The desired signal is at $\theta_d=20^0$, and SNR=0 dB. Two curves of output SINR versus θ_i are shown, for INR=0 dB and INR=20 dB. It may be seen that the SINR drops not only when θ_i is near 20^0, because the desired signal falls in the interference null, but also for θ_i near -41.1^0, when the desired signal falls in the grating null. The SINR drops to the same value for either $\theta_i=20^0$ or $\theta_i=-41.1^0$, because for isotropic elements the interference null and the grating null have the same depth.

Now let us add the element patterns to the problem. In this paper, we will assume each element has a dipole pattern,** with the two pattern maxima pointing in different directions. Specifically, we assume

$$f_1(\theta) = \cos(\theta-\theta_o - \tfrac{\alpha}{2}) \ , \tag{21a}$$

and

$$f_2(\theta) = \cos(\theta-\theta_o + \tfrac{\alpha}{2}) \ . \tag{21b}$$

---

*With only 2 elements, we will drop the subscript in d_2 - the distance between elements is simply d.

**By a "dipole pattern," we mean the pattern of a short dipole. Also, we ignore the effects of mutual impedances here.

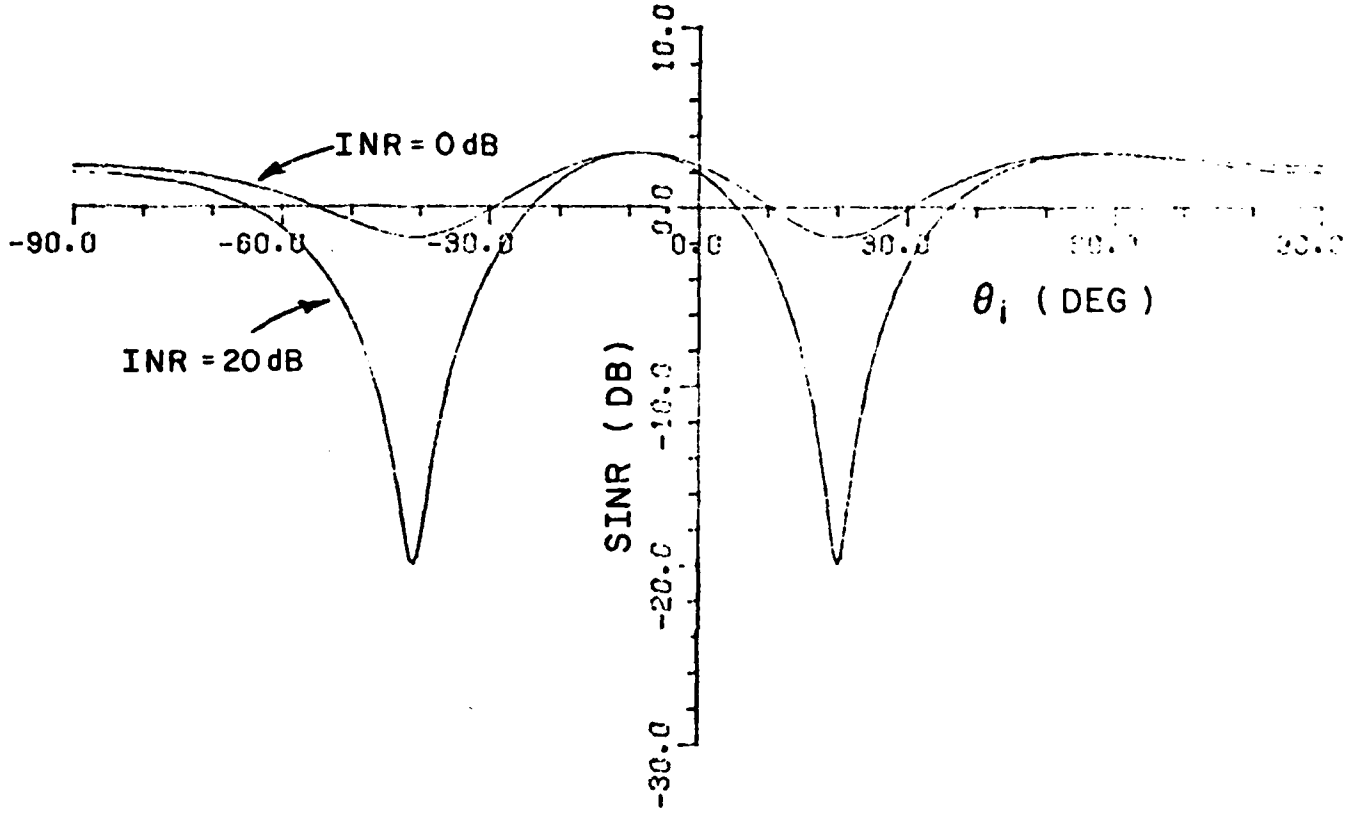

Figure 2. Output SINR vs θ_i for isotropic elements.
$d=1\lambda$, $\theta_d=20^o$, SNR=0 dB.

The beam maximum for element 1 is at $\theta=\theta_0+\frac{\alpha}{2}$ and that for element 2 is at $\theta=\theta_0-\frac{\alpha}{2}$. This situation is depicted in Figure 3.

Suppose first that both element patterns peak at broadside, i.e., $\alpha=\theta_0=0$ in Equation (21). Figure 4 shows the output SINR for SNR=0 dB, $\theta_d=20^0$, INR=20 dB and $d=\lambda$. The performance is similar to that for isotropic elements, except that the output SINR does not drop as far when $\theta_i=-41.1^0$. The reason is that with dipole patterns, the power of an interference signal at -41.1^0 is reduced by the element response. With less interference power coming into the array, the null produced at -41.1^0 is not as deep,* and hence the grating null at 20^0 is also not as deep.

Next consider the case where $\alpha\neq0$, but $\theta_0=0$, so the beam maxima are displaced symmetrically from broadside. Figures 5a-e show the output SINR for $\alpha=30^0$, 60^0, 90^0, 120^0 and 150^0 (and for SNR=0 dB, $\theta_d=20^0$ and INR=20 dB). By comparing these figures with Figure 4, it is seen that grating null effects are not as severe when $\alpha\neq0$. The reason is that when the element patterns are not identical, a weight vector that produces a null at -41.1^0 does not produce as deep a null at 20^0. (A signal at -41.1^0 has the same interelement phase shift as one at 20^0, but the amplitude ratios of the element signals are not the same at the two angles.) We see in Figures 5a-e that the grating null effect for $\theta_i=-41.1^0$ becomes progressively less important as α increases, i.e., as the patterns become less similar.

---

*In the LMS array, null depths vary with interference power [4].

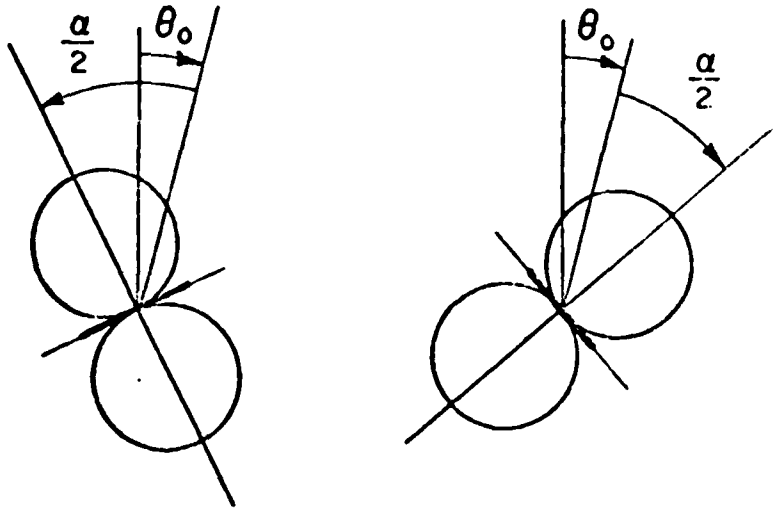

Figure 3. Dipole element patterns.

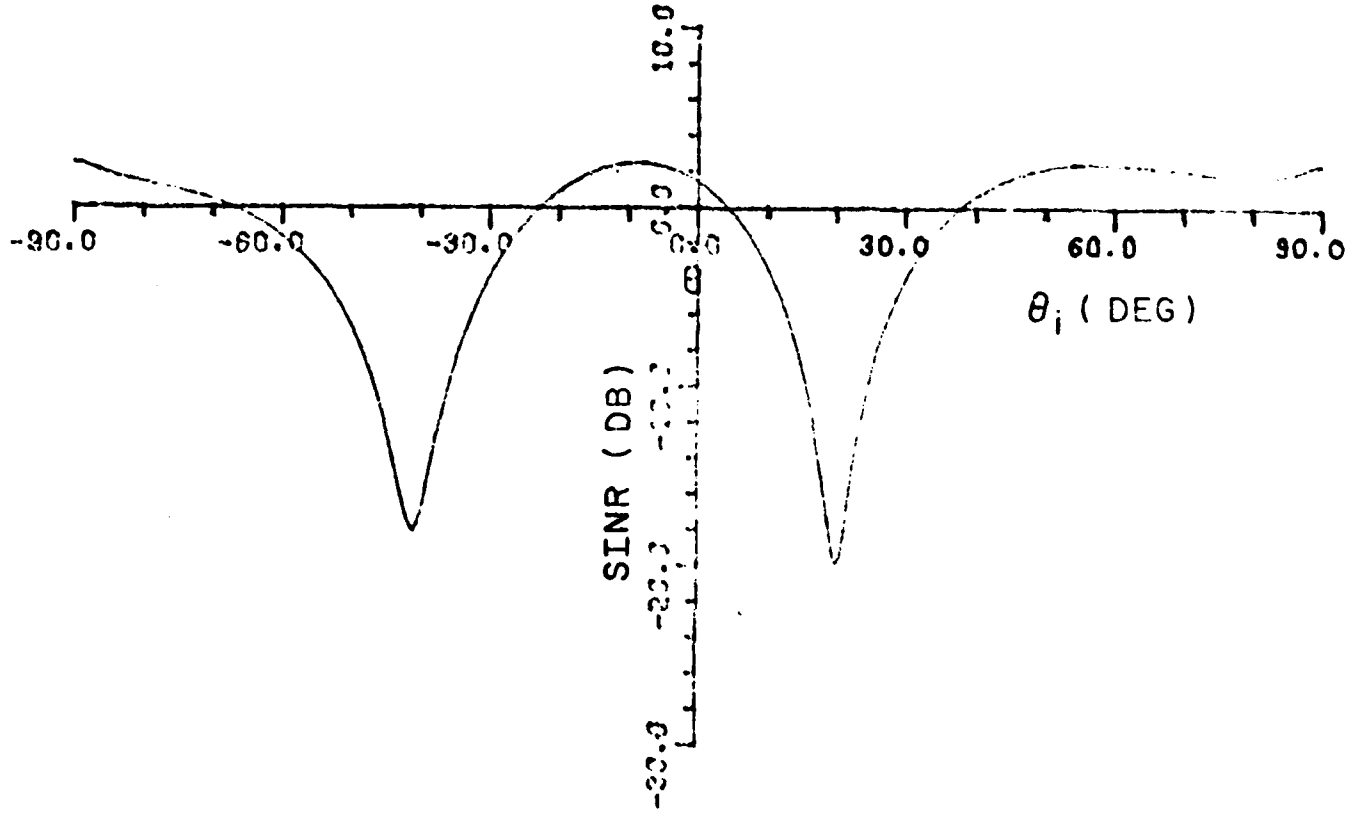

Figure 4. SINR vs θ_i. $\theta_o=0^o$, $\alpha=0^o$, $d=\lambda$, $\theta_d=20^o$, SNR=0 dB, INR=20 dB.

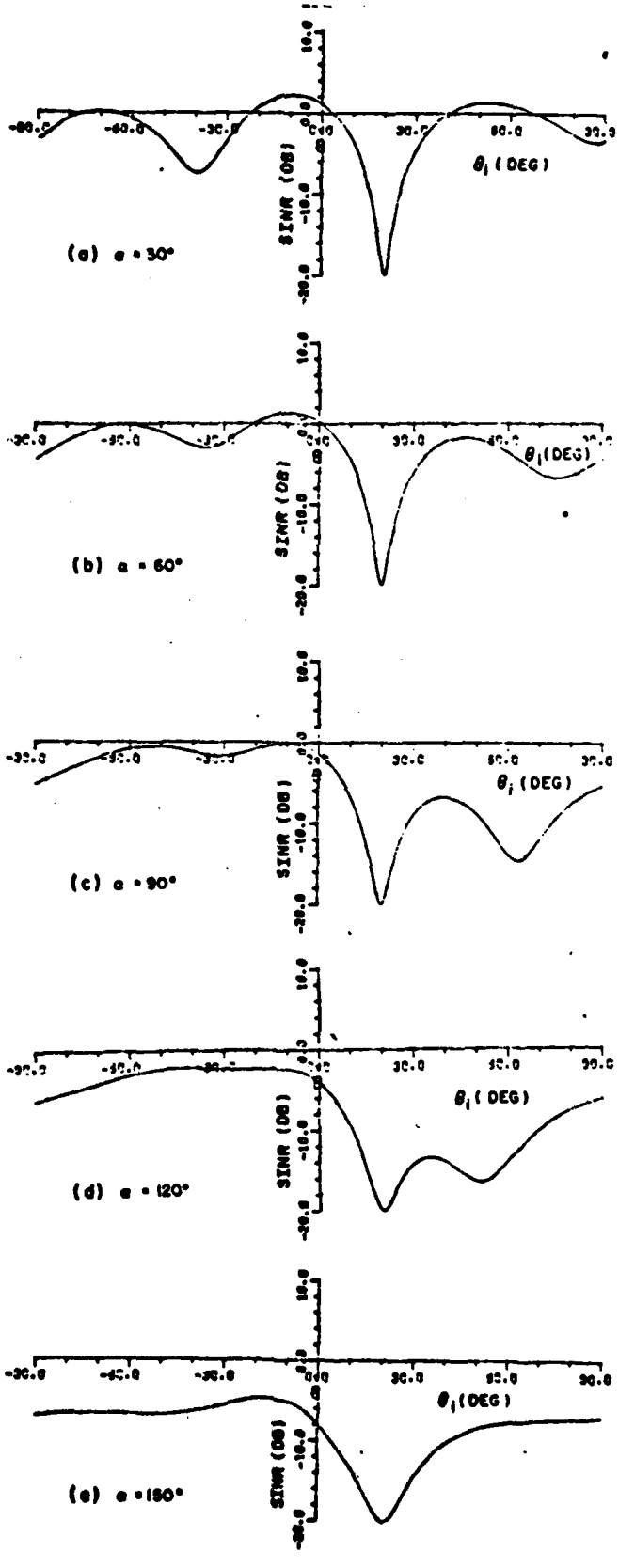

Figure 5. SINR vs θ_i. $\theta_0=0^0$, $d=\lambda$, $\theta_d=20^0$, SNR=0 dB, and INR=20 dB.

However, Figures 5a-e also show another effect. As α increases, although the performance near θ_i=-41.1^0 improves, a second region appears where the performance is poor. For example, when α=90^0, Figure 5c shows that the output SINR will be low if θ_i is near 63^0. For α=120^0 (Figure 5d), the performance is bad near θ_i=50^0. For α=150^0 (Figure 5e), the region of poor performance appears to have merged with the one for $\theta_i=\theta_d$, causing the width of this region to increase. A calculation of the angles in these cases shows that this effect is not due to a grating null as defined in Equation (20).

This extra "bad" angle occurs because, at this value of θ_i, one of the element patterns has changed sign but the other has not. As a result, a different interelement phase shift is now required to create a spurious null at θ_d.

Let us determine the conditions under which these grating nulls will occur. To do this, we note that a grating null will occur whenever the desired signal vector U_d is parallel to the interference vector U_i, i.e., whenever

$$U_d = KU_i, \tag{22}$$

where K is a constant. This statement is easily verified by noting that if Equation (22) holds, a weight vector chosen to null the interference,

$$w^T X_i = A_i e^{j(\omega_o t+\psi_i)}(w^T U_i) = 0, \tag{23a}$$

will also null the desired signal,

$$w^T X_d = A_d e^{j(\omega_o t+\psi_d)}(w^T U_d) = 0. \tag{23b}$$

Of course, Equation (22) is automatically satisfied when the interference arrives from the same angle as the desired signal. However, it may also be satisfied in other situations, with $\theta_d \neq \theta_i$, in which case the array will have grating null problems.

Consider the different ways Equation (22) may be satisfied. For the 2-element array, Equation (22) is equivalent to

$$\frac{f_1(\theta_d)}{f_2(\theta_d)e^{-j\phi_{d2}}} = \frac{f_1(\theta_i)}{f_2(\theta_i)e^{-j\phi_{i2}}} \quad . \tag{24}$$

For isotropic elements, with $f_1(\theta) = f_2(\theta) = 1$, this relationship will be satisfied if

$$\phi_{i2} = \phi_{d2} + 2n\pi, \quad n=0,\pm1,\pm2, \ldots, \tag{25}$$

which is equivalent to

$$\frac{2\pi d}{\lambda} \sin\theta_i = \frac{2\pi d}{\lambda} \sin\theta_d + 2n\pi, \tag{26}$$

i.e., the conventional grating null condition in Equation (20). An example of the array behavior in this case was shown in Figure 2.

For nonisotropic but identical element patterns, we have, for all θ,

$$f_1(\theta) = f_2(\theta), \tag{27}$$

so Equation (24) again yields the same grating null condition given in Equation (20). An example of this case was given in Figure 4.

For the more interesting case of nonisotropic and nonidentical element patterns, there are two ways to satisfy Equation (24). First, we may have

$$\frac{f_1(\theta_d)}{f_2(\theta_d)} = \frac{f_1(\theta_i)}{f_2(\theta_i)}, \tag{28a}$$

and

$$e^{j\phi_{d2}} = e^{j\phi_{i2}}. \tag{28b}$$

Equation (28b) is again the conventional grating null condition in Equation (20). To get the same null depth at θ_d as at θ_i, however, we must also satisfy Equation (28a). Typically, with unequal element patterns, when θ_i is at a grating null angle, Equation (28a) is not satisfied. If it is approximately satisfied, there will be a null near θ_d, but this null is not as deep as when Equation (28a) holds exactly. In this case the drop in output SINR for θ_i near the critical angle is not as great. Figure 5a is an example of this situation.

The second way to satisfy Equation (24) is with the pair of conditions,

$$\frac{f_1(\theta_d)}{f_2(\theta_d)} = -\frac{f_1(\theta_i)}{f_2(\theta_i)}, \tag{29a}$$

and

$$e^{j\phi_{d2}} = -e^{j\phi_{i2}}. \tag{29b}$$

Equation (29b) requires

$$\frac{2\pi d}{\lambda}\sin\theta_i = \frac{2\pi d}{\lambda}\sin\theta_d + (2n+1)\pi, \quad n=0,\pm1,\pm2,\ldots, \tag{30}$$

which yields a new set of critical angles for θ_i, different than those

in Equation (20). The drop in SINR that occurs when $\theta_i \sim 63^o$ in Figure 5c is due to a situation of this type. Again, how far the SINR drops when θ_i satisfies Equation (29b) depends on how closely Equation (29a) is satisfied at that angle. To obtain a solution to Equation (29a) requires that one element pattern have the same sign at θ_d and θ_i and the other have opposite signs at θ_d and θ_i. Because one element pattern must change sign between θ_d and θ_i, we will refer to grating nulls associated with this condition as "sign reversal" grating nulls. Grating nulls that occur when Equation (28) is satisfied will be referred to as conventional grating nulls.

Now let us consider in more detail the conditions under which conventional and sign reversal grating nulls will occur for the specific element patterns defined in Equations (21). We will start with the assumption that $d=\lambda$. (Also, we assume the signals may arrive from any angle within $(-\frac{\pi}{2}, \frac{\pi}{2})$.

Consider first conventional grating nulls as defined in Equation (28). Figure 6 shows the value of θ_i satisfying Equation (28b) for any given value of θ_d. If $\alpha=0$, then $f_1(\theta)=f_2(\theta)$, so Equation (28a) is satisfied for all θ_d, θ_i. If $\alpha\neq 0$, Equation (28a) is satisfied only for

$$\theta_i = \theta_d + n\pi, \quad n=0,\pm 1,\pm 2, \ldots, \tag{31}$$

which, for any given $\theta_d \varepsilon (-\frac{\pi}{2}, \frac{\pi}{2})$ and $n\neq 0$, lies outside the range $(-\frac{\pi}{2}, \frac{\pi}{2})$. Thus, with $\alpha=0$, any (θ_d,θ_i) on the curves in Figure 6 will yield a grating null condition, But with $\alpha\neq 0$, there are no sets of angles (θ_d,θ_i) in the range $(-\frac{\pi}{2}, \frac{\pi}{2})$ that satisfy both Equations (28a) and (28b). Strictly speaking, with $\alpha\neq 0$, there are no grating

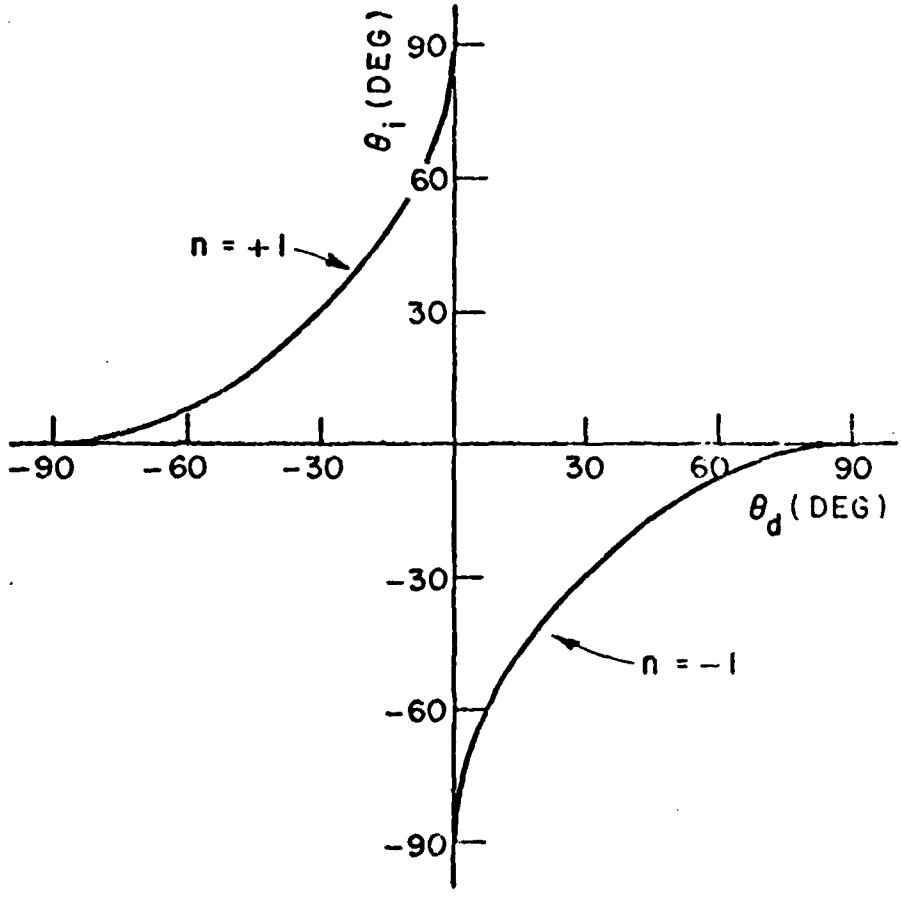

Figure 6. θ_i vs θ_d for grating null condition. (d=λ).

$$\frac{2\pi d}{\lambda} \sin\theta_i = \frac{2\pi d}{\lambda} \sin\theta_d + 2n\pi.$$

null solutions. Of course, in reality, if α is small, Equations (28) may be approximately satisfied at certain angles, so some grating null effects still occur. (Figure 5a illustrates this situation.)

Now consider the solutions to Equations (29). Figure 7 shows two sets of curves. The dashed curves show the values of θ_i satisfying Equation (29b) for any given θ_d and n. The solid curves are the solution to Equation (29a) for the case θ_o=0. Several curves are shown for different values of α. Any point (θ_d,θ_i) at which a solid curve and a dashed curve intersect defines a pair of angles at which the array will experience grating null problems.

The curves in Figure 7 are for $\theta_o=0^o$. (The beam maxima of the two element patterns are displaced symmetrically from broadside.) The effect of changing θ_o is to shift the solid curves in Figure 7 parallel to a 45^o line (a $\theta_i=\theta_d$ line) in the figure. For example, Figure 8 shows a set of curves for $\theta_o=30^o$. Note that in this case the curves satisfying Equation (29a) also intersect with curves satisfying Equation (29b) for n=1 and n=-2, so that a number of additional grating null angles now occur that were not present with $\theta_o=0^o$.

Finally, we note that changing the element spacing d changes the separation between the dashed curves in these figures. For example, Figure 9 shows the family of curves that result when $d=2\lambda$. Obviously, as d is increased, there will be more and more sets of critical angles.

It is clear from these curves that a two-element array with dipole element patterns will always experience grating nulls for any values of α and θ_o, as long as $d > \lambda/2$. The only way to avoid these nulls is to have $d \leq \lambda/2$ and $\theta_o=0$. Note also that for $\alpha\neq 0$, if $\theta_o\neq 0$

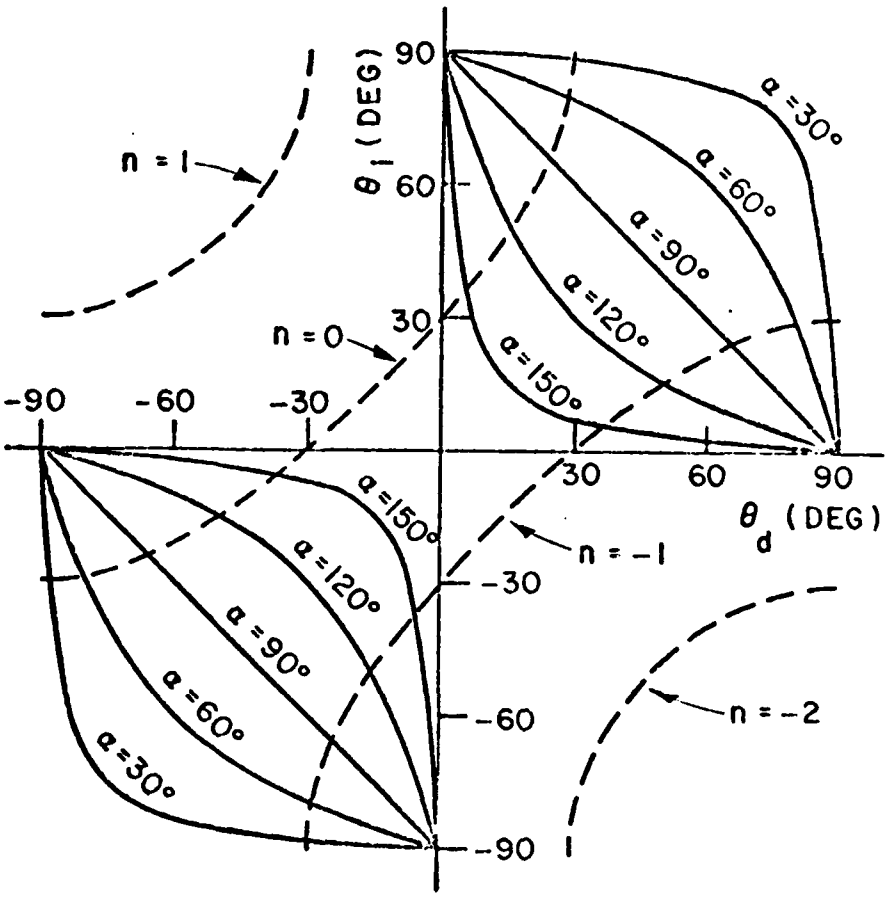

Figure 7. θ_i vs θ_d satisfying

$$(1) \quad \frac{2\pi d}{\lambda} \sin\theta_i = \frac{2\pi d}{\lambda} \sin\theta_d + (2n+1)\pi$$

$$(2) \quad \frac{\cos(\theta_d + \frac{\alpha}{2})}{\cos(\theta_d - \frac{\alpha}{2})} = -\frac{\cos(\theta_i + \frac{\alpha}{2})}{\cos(\theta_i - \frac{\alpha}{2})}$$

for $\theta_0 = 0^0$, $d = \lambda$.

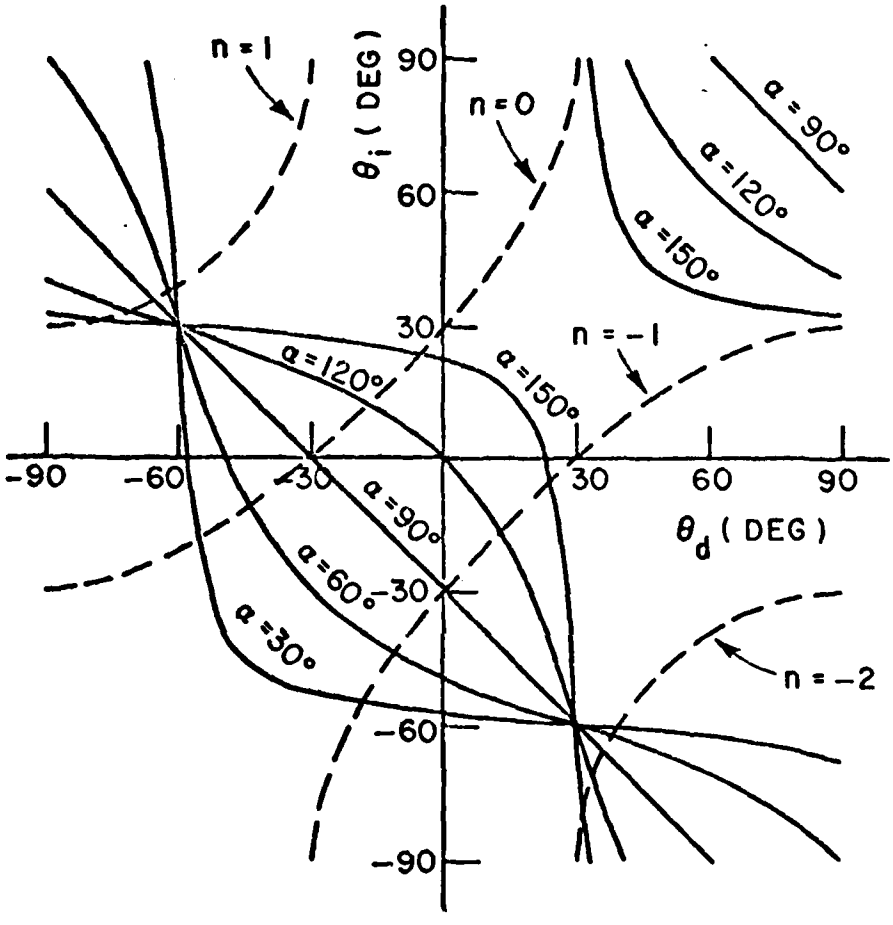

Figure 8. θ_i vs θ_d satisfying

$$(1) \quad \frac{2\pi d}{\lambda} \sin\theta_i = \frac{2\pi d}{\lambda} \sin\theta_d + (2n+1)\pi$$

and

$$(2) \quad \frac{\cos(\theta_d - \theta_o + \frac{\alpha}{2})}{\cos(\theta_d - \theta_o - \frac{\alpha}{2})} = -\frac{\cos(\theta_i - \theta_o + \frac{\alpha}{2})}{\cos(\theta_i - \theta_o - \frac{\alpha}{2})}$$

for $\theta_o = 30^o$, $d = \lambda$

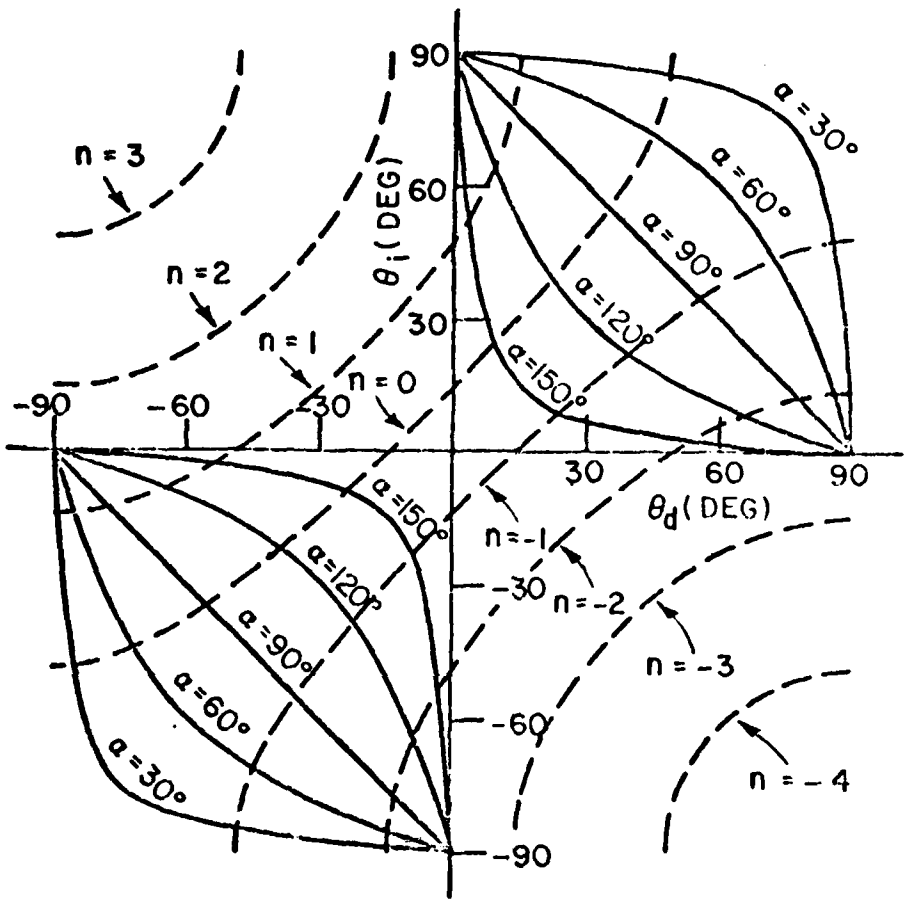

Figure 9. θ_i vs θ_d satisfying

$$(1) \quad \frac{2\pi d}{\lambda} \sin\theta_i = \frac{2\pi d}{\lambda} \sin\theta_d + (2n+1)\pi$$

and

$$(2) \quad \frac{\cos(\theta_d + \frac{\alpha}{2})}{\cos(\theta_d - \frac{\alpha}{2})} = -\frac{\cos(\theta_i + \frac{\alpha}{2})}{\cos(\theta_i - \frac{\alpha}{2})}$$

for $d = 2\lambda$

sign reversal grating nulls occur even if $d < \lambda/2$! (For $d = \lambda/2$, for example, solving Equation (30) for θ_i vs. θ_d yields the same curve as shown in Figure 6. This curve will intersect some of the solid curves in Figure 8.)

We conclude from all of this that it is impossible to avoid grating null problems with two elements having dipole patterns if $d > \lambda/2$. If $\alpha=0$ and $\theta_o=0$, grating null effects such as shown in Figure 4 occur, and if $\alpha\neq 0$, sign reversal grating nulls always occur.

Fortunately, grating null problems appear to be less severe if more than two elements are used. In the next section, we discuss the reason that additional elements are helpful and illustrate what can be done with a three-element array.

IV. A THREE-ELEMENT ARRAY

With more than two elements, it is possible to find combinations of element patterns for wide spacing that eliminate grating null problems. We first make some general remarks about the reasons for the difference and then show an example.

Assume we have a three-element array with one-wavelength spacing ($d_2=\lambda, d_3=2\lambda$). Let the jth element have the pattern

$$f_j(\theta) = \cos(\theta-\alpha_j). \tag{32}$$

Suppose we wish to choose the α_j so grating null effects are minimized.

To prevent grating nulls, we must assure that the vectors U_d and U_i do not become parallel for any combination of θ_d and θ_i (except $\theta_d=\theta_i$) over the sector of interest. One way to do this is to choose the α_j so the quantity

$$F(\theta_d,\theta_i,K) = |U_d-KU_i|^2 \tag{33}$$

is nonzero for all (θ_d,θ_i), and for all values of the constant K. For any given θ_d and θ_i, the value of K that minimizes $F(\theta_d,\theta_i,K)$ is

$$K = \frac{U_d^T U_i^*}{U_i^T U_i^*} . \tag{34}$$

(set $\partial F/\partial K = 0$). The value of F for this K, which we call $I(\theta_d,\theta_i)$ is

$$I(\theta_d,\theta_i) = \min_K F(\theta_d,\theta_i,K) = U_d^T U_d^* - \frac{(U_d^T U_i^*)(U_i^T U_d^*)}{U_i^T U_i^*} . \tag{35}$$

We may view $I(\theta_d,\theta_i)$ as a performance index that, to prevent grating nulls, should be nonzero for all θ_d,θ_i.*

For a three element array, we substitute

$$U_d = \begin{pmatrix} f_1(\theta_d) \\ f_2(\theta_d)e^{-j\phi_{d2}} \\ f_3(\theta_d)e^{-j\phi_{d3}} \end{pmatrix} \tag{36a}$$

$$U_i = \begin{pmatrix} f_1(\theta_i) \\ f_2(\theta_i)e^{-j\phi_{i2}} \\ f_3(\theta_i)e^{-j\phi_{i3}} \end{pmatrix} \tag{36b}$$

---

*Note that $I(\theta_d,\theta_i)$ has the same dependence on θ_d and θ_i as the SINR in Equation (18), as long as $\xi_i^{-1} \ll U_i^T U_i^*$, i.e., as long as the interference-to-noise ratio is high.

into Equation (35). The resulting expression may be manipulated into the form:

$$I(\theta_d, \theta_i) = \frac{|D_{12}|^2 + |D_{13}|^2 + |D_{23}|^2}{\sum_{k=1}^{3} |f_k(\theta_i)|^2} , \tag{37a}$$

where D_{nm} is the determinant*

$$D_{nm} = \begin{vmatrix} f_n(\theta_d)e^{-j\phi_{dn}} & f_n(\theta_i)e^{-j\phi_{in}} \\ f_m(\theta_d)e^{-j\phi_{dm}} & f_m(\theta_i)e^{-j\phi_{im}} \end{vmatrix} . \tag{37b}$$

Since the numerator of $I(\theta_d,\theta_i)$ contains the sum of the magnitude-squared value of three determinants D_{nm}, the only way for $I(\theta_d,\theta_i)$ to be zero is for all three D_{nm} to be zero at the same (θ_d,θ_i). But for a given D_{nm} to be zero requires the two vectors

$$\begin{pmatrix} f_n(\theta_d)e^{-j\phi_{dn}} \\ f_m(\theta_d)e^{-j\phi_{dm}} \end{pmatrix} \quad \text{and} \quad \begin{pmatrix} f_n(\theta_i)e^{-j\phi_{in}} \\ f_m(\theta_i)e^{-j\phi_{im}} \end{pmatrix}$$

to be linearly dependent. However, this is just the condition for the two-element array consisting of the nth and mth elements to have a grating null problem at the given (θ_d, θ_i), as discussed in Section III. To have $I(\theta_d, \theta_i)=0$ with the three-element array then requires that D_{12}, D_{13} and D_{23} all be zero at the <u>same set of angles</u> (θ_d, θ_i).

---

*ϕ_{d1} and ϕ_{i1} are used in Equation (37b) for notational convenience, but are zero by definition.

I.e., all two-element pairs taken from the three-element array must have the same grating null angles. This observation makes it clear why one can avoid grating nulls with three elements, because it is easy to arrange a three-element array so the critical angles for the three element pairs are not the same. Then when one D_{nm} term in Equation (37a) is zero, the other two are not, and $I(\theta_d,\theta_i)$ is never zero.

Figures 10a-g illustrate the type of performance that can be obtained with a three-element array having one wavelength element spacing and element patterns as given in Equation (32). These calculations are for $d_2=\lambda$, $d_3=2\lambda$, $\alpha_1=-60^0$, $\alpha_2=0^0$, $\alpha_3=60^0$, SNR=0 dB and INR=40 dB. The figures show the SINR as a function of θ_i for several values of θ_d. It is seen that grating nulls have been avoided with this choice of parameters.

The α_i's used in Figure 10 were obtained by trial-and-error, and were selected to give good overall performance without grating nulls. However, it is not known whether this choice is optimum in some sense or not. In fact, choosing the α_j (and possibly d_j) to optimize an array design appears to be a difficult task. In this report, we do not discuss the optimization problem.

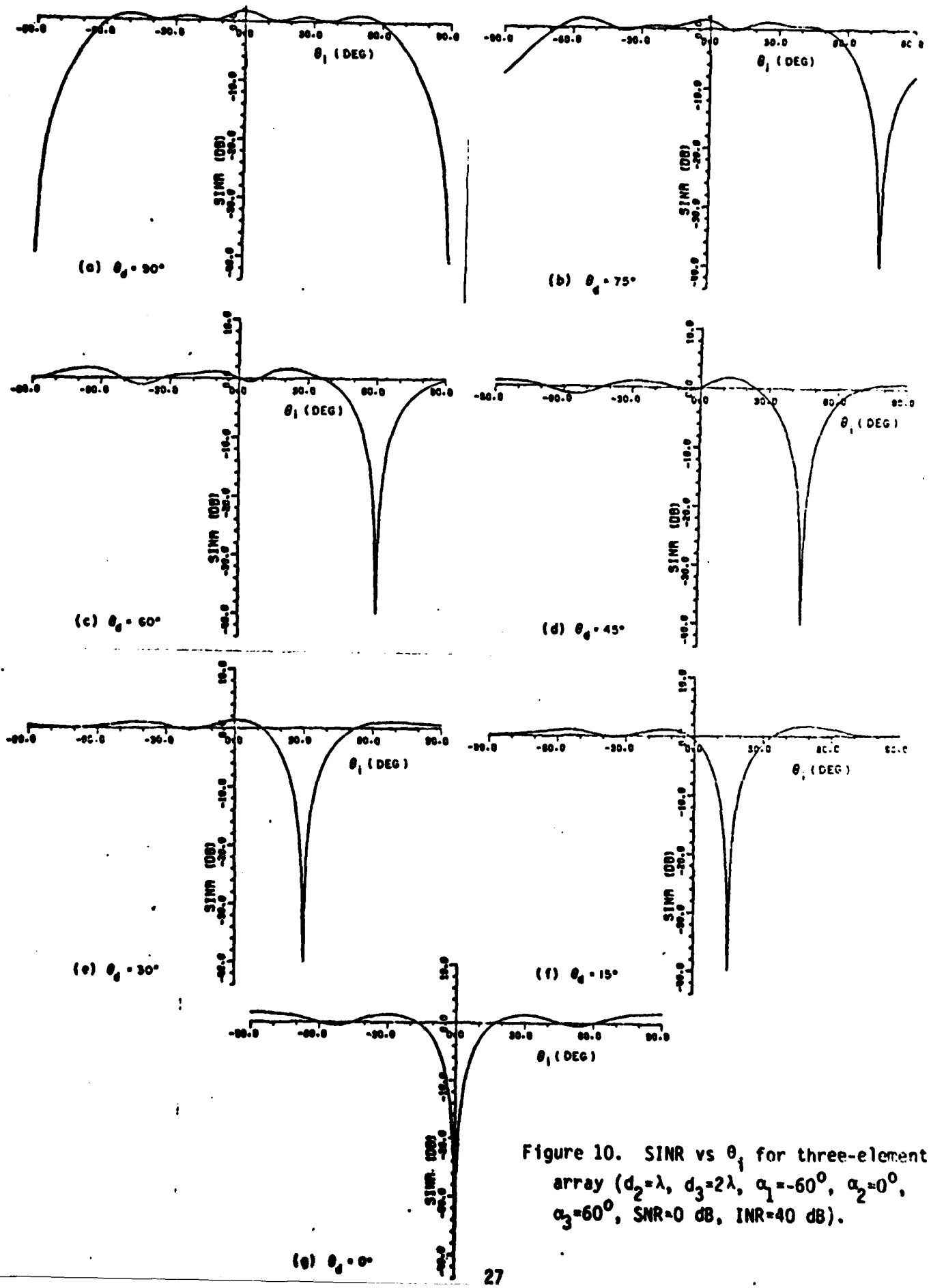

Figure 10. SINR vs θ_i for three-element array ($d_2=\lambda$, $d_3=2\lambda$, $\alpha_1=-60^0$, $\alpha_2=0^0$, $\alpha_3=60^0$, SNR=0 dB, INR=40 dB).

V. CONCLUSIONS

We have shown that element patterns in an adaptive array have a large effect on the grating null performance of the array. We have found that the element patterns can cause extra grating nulls ("sign reversal grating nulls"), in addition to conventional grating nulls. For a two-element array with dipole element patterns, it was shown that grating nulls cannot be avoided with element spacing larger than a half wavelength. Moreover, sign reversal grating nulls occur even with spacings less than a half wavelength if the element patterns are not properly chosen.

With more than two elements in the array, however, it is possible to overcome grating nulls by choosing the element patterns appropriately. An example was given with three dipole elements one wavelength apart in which no grating nulls occur.

VI. APPENDIX

The purpose of this appendix is to derive Equation (18) from Equation (14). The first step in this derivation is to determine the weight vector in Equation (1), where Φ is given by (see Equation (9)):

$$\Phi = \sigma^2 I + A_d^2 U_d^* U_d^T + A_i^2 U_i^* U_i^T \ . \tag{A-1}$$

To find Φ^{-1}, we make use of the following matrix inversion lemma,

$$(B-\beta Z^* Z^T)^{-1} = B^{-1} - \tau B^{-1} Z^* Z^T B^{-1} \ , \tag{A-2}$$

where B is a nonsingular NxN matrix, Z is an Nx1 column vector, and β and τ are scalars related by

$$\tau^{-1} + \beta^{-1} = Z^T B^{-1} Z^* \ . \tag{A-3}$$

We start by using this lemma on the matrix $\sigma^2 I + A_i^2 U_i^* U_i^T$. We find

$$(\sigma^2 I + A_i^2 U_i^* U_i^T)^{-1} = \frac{1}{\sigma^2}\left[1 - \frac{U_i^* U_i^T}{\xi_i^{-1} + U_i^T U_i^*}\right] . \tag{A-4}$$

(ξ_i is defined in Equation (19b).) Then by letting $B = \sigma^2 I + A_i^2 U_i^* U_i^T$, $Z = U_d$ and $\beta = -A_d^2$, we use the lemma again to find

$$\Phi^{-1} = \frac{1}{\sigma^2} I - \frac{\tau}{\sigma^4} U_d^* U_d^T - \frac{1}{\xi_i^{-1} + U_i^T U_i^*}\left[\frac{1}{\sigma^2} + \frac{\tau}{\sigma^4}\frac{(U_i^T U_d^*)(U_d^T U_i^*)}{\xi_i^{-1} + U_i^T U_i^*}\right] U_i^* U_i^T$$

$$+ \frac{\tau}{\sigma^4}\frac{(U_d^T U_i^*)}{\xi_i^{-1} + U_i^T U_i^*} U_d^* U_i^T + \frac{\tau}{\sigma^4}\frac{U_i^T U_d^*}{\xi_i^{-1} + U_i^T U_i^*} U_i^* U_d^T \ , \tag{A-5}$$

where

$$\tau^{-1} = \frac{1}{A_d^2} + \frac{1}{\sigma^2} U_d^T U_d^* - \frac{1}{\sigma^2}\left[\frac{(U_d^T U_i^*)(U_i^T U_d^*)}{\xi_i^{-1} + U_i^T U_i^*}\right] . \tag{A-6}$$

It is helpful to define the quantity

$$\gamma = A_d^2\left[U_d^T U_d^* - \frac{(U_i^T U_d^*)(U_d^T U_i^*)}{\xi_i^{-1} + U_i^T U_i^*}\right] , \tag{A-7}$$

and then Equation (A-6) may be written

$$\tau = A_d^2\left(1 + \frac{\gamma}{\sigma^2}\right)^{-1} . \tag{A-8}$$

Now multiplying Φ^{-1} in Equation (A-5) onto S in Equation (13), we have

$$w = \Phi^{-1} A_r A_d U_d^*, \tag{A-9}$$

which simplifies to

$$w = \frac{A_r A_d}{\sigma^2}\left(1 - \frac{\tau}{\sigma^2}\frac{\gamma}{A_d^2}\right)\left(U_d^* - \frac{U_i^T U_d^*}{\xi_i^{-1} + U_i^T U_i^*} U_i^*\right) . \tag{A-10}$$

Next we find

$$U_d^T w = \frac{A_r A_d}{\sigma^2}\left(1 - \frac{\tau}{\sigma^2}\frac{\gamma}{A_d^2}\right)\frac{\gamma}{A_d^2} , \tag{A-11}$$

or, after substituting Equation (A-8) for τ,

$$U_d^T w = \frac{A_r}{A_d}\left(\frac{\gamma}{\sigma^2 + \gamma}\right) . \tag{A-12}$$

Therefore, from Equation (15), the output desired signal power is

$$P_d = \frac{A_d^2}{2} |U_d^T w|^2 = \frac{A_r^2}{2}\left(\frac{\gamma}{\sigma^2+\gamma}\right)^2 . \tag{A-13}$$

Similarly, we find

$$U_i^T w = \frac{A_r A_d}{\sigma^2}\left(1 - \frac{\tau}{\sigma^2}\,\frac{\gamma}{A_d^2}\right) U_i^T U_d^* \left(\frac{\xi_i^{-1}}{\xi_i^{-1}+U_i^T U_i^*}\right) , \tag{A-14}$$

so, from Equation (16)

$$P_i = \frac{A_i^2}{2}|U_i^T w|^2$$

$$= \frac{A_r^2 A_d^2 A_i^2}{2}\left(\frac{1}{\sigma^2+\gamma}\right)^2\left(\frac{\xi_i^{-1}}{\xi_i^{-1}+U_i^T U_i^*}\right)^2 (U_i^T U_d^*)(U_d^T U_i^*). \tag{A-15}$$

Finally, from Equation (A-10), we have

$$|w|^2 = A_r^2 A_d^2\left(\frac{1}{\sigma^2+\gamma}\right)^2\left[\frac{\gamma}{A_d^2} - (U_d^T U_i^*)(U_i^T U_d^*)\,\frac{\xi_i^{-1}}{(\xi_i^{-1}+U_i^T U_i^*)^2}\right] , \tag{A-16}$$

so from Equation (17),

$$P_n = \frac{A_r^2 A_d^2 A_i^2}{2}\left(\frac{1}{\sigma^2+\gamma}\right)^2\left\{\frac{\gamma\xi_i^{-1}}{A_d^2} - (U_d^T U_i^*)(U_i^T U_d^*)\left(\frac{\xi_i^{-1}}{\xi_i^{-1}+U_i^T U_i^*}\right)^2\right\}. \tag{A-17}$$

Combining Equations (A-15) and (A-17) gives

$$P_i+P_n = \frac{A_r^2 A_i^2}{2}\left(\frac{1}{\sigma^2+\gamma}\right)^2 \gamma\xi_i^{-1}. \tag{A-18}$$

Then using Equation (A-13) for P_d, we find that the SINR reduces to the remarkably simple form

$$SINR = \frac{P_d}{P_i + P_n} = \frac{\gamma}{\sigma^2} . \qquad (A\text{-}19)$$

From the definition of γ in Equation (A-7), we see that this result is the same as Equation (18).

REFERENCES

1. B. Widrow, P. E. Mantey, L. J. Griffiths and B. B. Goode,"Adaptive Antenna Systems," Proc. IEEE, 55, p. 2143, December 1967.
2. R. T. Compton, Jr., "The Power Inversion Adaptive Array - Concept and Performance," IEEE Trans. Aerospace and Electronic Systems, vol. AES-15, p. 803, November, 1979.
3. R. L. Riegler and R. T. Compton, Jr., "An Adaptive Array for Interference Rejection," Proc. IEEE, vol. 61, p. 748, June 1973.
4. R. T. Compton, Jr., "An Experimental Four-Element Adaptive Array," IEEE Trans. Antennas and Propagation, vol. AP-24, p. 697, September 1976.
5. R. T.Compton, Jr., R. J. Huff, W. G. Swarner and A. A. Ksienski, "Adaptive Arrays for Communication Systems: An Overview of Research at The Ohio State University," IEEE Trans. Antennas and Propagation, vol. AP-24, p. 599, September 1976.
6. R. T. Compton, Jr., "An Adaptive Array in a Spread-Spectrum Communication System," Proc. IEEE, vol. 66, p. 289, March 1978.